Check for updates

Physiologia Plantarum

SPPS

ORIGINAL RESEARCH OPEN ACCESS

Exploring Plant Surface Chemical Variability: Lettuce Leaf as Model

Ana Galindo-Bernabeu[1,2] | Giovanni Sáenz-Arce[1,3] | B. Santiago Guaillazaca-Gonzalez[4] | Tamara González-Illanes[5] | Chantal Ferrer-Roca[4] | Sonia Murcia-Mascarós[4] | Ana González Moreno[6] | Ana Cros[4] | Jaime Colchero[1] | Victoria Fernández[5]

[1]Centro de Investigación en Óptica y Nanofísica, Departamento de Física, Campus Espinardo, Universidad de Murcia, Murcia, Spain | [2]Universidad Técnica Nacional (UTN), Alajuela, Costa Rica | [3]Departamento de Física, Facultad de Ciencias Exactas y Naturales, Universidad Nacional, Heredia, Costa Rica | [4]Institut de Ciència dels Materials, Universitat de València, Paterna, Spain | [5]Department of Systems and Natural Resources, School of Forest Engineering, Technical University of Madrid, Madrid, Spain | [6]Instituto de Hortofruticultura Subtropical y Mediterránea "La Mayora", Universidad de Málaga, Málaga, Spain

Correspondence: Victoria Fernández (v.fernandez@upm.es)

Received: 24 April 2025 | **Accepted:** 30 September 2025

Handling Editor: E. Pesquet

Funding: This work was supported by the European Union NextGenerationEU/PRTR funds (TED2021-130830B-C41, TED2021-130830B-C42, TED2021-130830B-C43), the Ministerio de Ciencia e Innovación (PID2019-104272RB-C52, PID2022-139191OB-C31) and the Ministerio de Ciencia, Innovación y Universidades (PDC2023-145906-I00).

Keywords: cell wall | cuticle | nanoscale heterogeneity | plant surfaces | wettability

ABSTRACT

The plant cuticle has been traditionally believed to be a continuous lipophilic layer covering most aerial plant surfaces, but recent methodological advances based on Atomic Force Microscopy (AFM) enabled mapping the distribution of hydrophilic and hydrophobic areas in the papillae and pavement cells of rose petals and olive leaf trichomes. Since previous investigations associated the occurrence of foodborne diseases in leafy green vegetables with a high water wettability and stomatal traits, we hypothesised that lettuce could be a suitable model for a plant surface having a higher frequency of nano-hydrophilic areas. Hence, a wettable Romaine lettuce variety with water contact angles between 64° and 75° and a high degree of polarity for both leaf sides was selected and characterised by electron microscopy, AFM, Fourier Transform Infrared (FTIR) and Raman Spectroscopy. Leaf samples were analysed fresh and after critical point drying (CPD), and no major structural or chemical differences were recorded. Leaves are amphistomatous and were found to have nano-scale chemical heterogeneity in both leaf sides, with hydrophilic nano-areas predominantly occurring in stomatal regions. These hydrophilic nano-areas could facilitate microbial adhesion and affect transport phenomena across leaf surfaces, but the functional significance of hydrophilic nano-zones in the cuticle of aerial plant organs will need to be addressed in future multidisciplinary investigations.

1 | Introduction

Plant leaves are protected from an array of biotic and abiotic factors by an epidermis composed of cells of different shapes, sizes and functionalities (Chassot et al. 2007; Javelle et al. 2011; Riglet et al. 2021). The outermost layer of epidermal cells, which is in contact with the surrounding environment, is named cuticle (Jeffree 2006; Lequeu et al. 2003). This protective layer can be considered a cell wall with variable amounts of lipids (Guzmán et al. 2014; Segado et al. 2016; Heredia et al. 2024). The cuticle is a composite material made of hydrophobic (cutin polyester and waxes) and hydrophilic (cell wall polysaccharides)

This is an open access article under the terms of the Creative Commons Attribution-NonCommercial-NoDerivs License, which permits use and distribution in any medium, provided the original work is properly cited, the use is non-commercial and no modifications or adaptations are made.

© 2025 The Author(s). *Physiologia Plantarum* published by John Wiley & Sons Ltd on behalf of Scandinavian Plant Physiology Society.

constituents (Fernández et al. 2016). Many aerial surfaces have a layer of epicuticular waxes deposited onto the cuticle surface, while intracuticular waxes are located in the cuticle interior (Dominguez et al. 2011; Jeffree 2006; Veličković et al. 2014). Cuticular waxes include a complex mixture of compounds of different chain lengths, such as alkanes, alcohols, aldehydes, ketones or esters (Jetter and Riederer 2016; Zeisler-Diehl et al. 2018; Patwari et al. 2019; Dang and Suh 2025). Cutin polyester is composed of C_{16} and/or C_{18} fatty acids, with one or more hydroxyl, mid-chain epoxide and end-chain carboxyl functional groups (Dominguez et al. 2011; Yeats and Rose 2013; Philippe et al. 2020). The innermost part of the cuticle adjacent to the cell wall is rich in polysaccharides (cellulose, hemicellulose and pectin; Jeffree 2006; Heredia-Guerrero et al. 2014; Segado et al. 2016). Minor amounts of polyphenols, such as flavonoids or cinnamic acids, can also be found in the cuticle (Karabourniotis and Liakopoulos 2006; Moreno et al. 2023). Cuticular chemical and structural diversity has been reported when attempting to establish taxonomic cuticle comparisons (Yeats et al. 2012), during seasons (Laoué et al. 2023), or in response to stress factors such as drought (Patwari et al. 2019; Dang and Suh 2025), pest (Kosma et al. 2010) or pathogen (Chassot et al. 2007; Isaacson et al. 2009) attack.

In the case of Romaine lettuce, the plant species analysed in this study, the most abundant epicuticular waxes may be alkanes, fatty acids and alcohols (Lu et al. 2015; Ku et al. 2020). On the other hand, chemical analyses of different lettuce varieties identified compounds such as chlorogenic, caffeic, p-coumaric or ferulic acids, the main flavonoids being quercetin and cyanidin glycosides (Zivcak et al. 2017).

Some studies performed during the last decade provided evidence for the chemical heterogeneity of the cuticle and the importance of cell wall polysaccharides (e.g., Guzmán et al. 2014; Segado et al. 2016; Philippe et al. 2020; Sasani et al. 2021; Moreno et al. 2023). For example, when analysing cell-type-specific differences in *Arabidopsis thaliana* leaves, Hegebarth et al. (2016) reported wax composition variations between trichomes and pavement cells. The occurrence of hydrophilic nano-areas in the cuticle covering papillae and pavement cells of rose petals (Almonte et al. 2022) and olive leaf trichomes (Fernández et al. 2024) has been recently reported.

To date, a major importance has been attributed to surface roughness, at least in terms of surface wettability and retention of water drops (e.g., Koch et al. 2008), but the occurrence of nano-scale surface chemical heterogeneity in the cuticle may have major physiological and functional implications that are currently unexplored. For example, cuticular water loss when stomata are closed (the so-called residual transpiration, Hasanuzzaman et al. 2023) may be increased by the occurrence of nano-hydrophilic areas, which may likely be associated with cuticle zones having lower amounts of lipids (Fernández et al. 2024). The surface features of epidermal cells may favour the retention and absorption of surface-deposited water (Schreel et al. 2020; Liu et al. 2023; Losso et al. 2023), agrochemicals or aerosols (Fernández et al. 2021).

Lettuce is an important horticultural commodity (Natesh et al. 2017; Zivcak et al. 2017; Dong et al. 2024) that is quite susceptible to pathogen contamination (Ku et al. 2020; Lu et al. 2015). In some studies on microbial contamination of leafy green vegetables, bacteria were often found in areas with low epicuticular wax coverage, in the abaxial leaf side where stomatal density is higher (Palma-Salgado et al. 2020; Truschi et al. 2023; Dong et al. 2024) or associated with hairs or specific chemical features (Beattie and Lindow 1999; Yadav et al. 2005). Pathogen attachment to leafy green surfaces has been related to the composition, density and morphology of epicuticular waxes (Lu et al. 2015; Chiu et al. 2020; Ku et al. 2020; Dong et al. 2024). Working with group A porcine rotavirus, Lu et al. (2015) observed that the occurrence of crystallised epicuticular waxes significantly inhibited viral adsorption to the surface of 24 leafy greens and tomato cultivars.

The structure and chemical composition of plant surfaces have an influence on multiple processes such as pathogen attachment, wettability and adhesion or repulsion of water drops or transport mechanisms across epidermal cell walls (Fernández et al. 2021). Leaf surface traits affecting wettability may vary upon factors such as organ side, age or growing conditions (Smith and McClean 1989; Brewer et al. 1991; Rosado and Holder 2013; Bei et al. 2023). Leaf wettability is affected by chemical composition and topography, but currently, there is limited information on the nano-scale distribution of cuticle hydrophilic and hydrophobic components (Almonte et al. 2022), which may have an important functional role. The significance of leaf surface wettability as an adaptation for optimising gas exchange and water use efficiency is unclear so far (Smith and McClean 1989; Brewer et al. 1991; Hanba et al. 2004). Adhesion or repulsion of atmospheric water due to, for example, rain, condensation or fog may enable or prevent foliar water and gas exchange across leaf surfaces and also affect water delivery to the roots (Rosado and Holder 2013; Fernández et al. 2021; Roth-Nebelsick et al. 2022; Bei et al. 2023). Furthermore, increased leaf surface roughness and poor wettability (i.e., very high water contact angles) have been associated with lower susceptibility to pathogen attachment and proliferation in various leafy greens (Lu et al. 2015; Truschi et al. 2023).

The plant cuticle is made of hundreds of chemical compounds arranged at the nano-scale, and technological constraints for elucidating their localisation currently limit our understanding of cuticle structure and composition (Fernández et al. 2016). Indeed, the relationship between macroscopic wettability, as estimated by contact angle determination, and nano-scale surface hydrophilicity–hydrophobicity remains unexplored to date. Hence, aware that lettuce leaves are wettable, as described above, we selected a Romaine lettuce variety under the hypothesis that its leaves may have a higher frequency of nano-hydrophilic areas compared to rose petals and olive leaves. In addition, the following hypotheses were tested with lettuce as a model for a plant organ with a higher presence of hydrophilic cuticular nano-areas: (i) adaxial and abaxial leaf surfaces have hydrophilic nano-zones, and (ii) there are epidermal cell-type specific differences regarding the occurrence of hydrophilic nano-zones in the cuticle.

2 | Materials and Methods

Experiments were developed with 20, approximately 3-month-old Romaine lettuce (*Lactuca sativa* L. var.

13993054, 2025, 5, Downloaded from https://onlinelibrary.wiley.com/doi/10.1111/ppl.70580 by Victoria Fernandez - Spanish Cochrane National Provision (Ministerio de Sanidad) , Wiley Online Library on [17/10/2025]. See the Terms and Conditions (https://onlinelibrary.wiley.com/terms-and-conditions) on Wiley Online Library for rules of use; OA articles are governed by the applicable Creative Commons License

'Turbina') grown from seedlings (Semilleros El Raal Cox S L., Alicante, Spain) in 1.3-L pots filled with perlite and compost, under greenhouse conditions (School of Forest Engineering, Technical University of Madrid, Spain) under 10–12 h light photoperiod, 15°C–25°C and 40%–80% relative humidity. During cultivation, plants were fertilised and managed to be free of pests and diseases, ensuring that the foliage was in a good state. In general, experiments were performed by collecting middle lamina sections of healthy, fully expanded leaves, with an average of 3–10 samples being collected from different leaves and plants depending on the technique to be applied. The upper (adaxial) and lower (abaxial) surfaces of intact, fresh (i.e., with no further preparation) lettuce leaves were directly analysed by AFM, SEM, FTIR and RAMAN spectroscopy.

For AFM, SEM, FTIR and RAMAN spectroscopy analyses, fresh and AFM, SEM, FTIR critical point-dried (CPD) tissues were examined. For CPD sample preparation, approximately 5 mm^2 sections from 10 different leaves, collecting three sections per leaf from a total of 10 plants (one leaf was sampled per plant; $N = 30$), were immediately immersed in phosphate buffer (7.2 pH) containing glutaraldehyde (2.5%) and paraformaldehyde (4%) (both from Electron Microscopy Sciences), keeping the samples at 4°C for 1.5 h. Fixed tissues were consequently rinsed four times (10 min each) in phosphate buffer before dehydration in a series of absolute ethanol (30%, 50%, 70%, 80%, 90%, 95% and 100%) (Merck). Solutions were changed twice (10 min each) until reaching a concentration of 70% ethanol (70%), which was kept for 12 h at 4°C. Leaf tissues were further dehydrated in 80, 90 and 100% ethanol (×2 times, 10 min each) and subjected to critical point drying (Leica EM CPD300).

2.1 | Scanning Electron Microscopy

The adaxial and abaxial sides of five fresh (one leaf per plant and a total of five plants sampled) and five CPD lettuce leaf sections were directly observed (analysing three different areas per leaf piece) by field emission scanning electron microscopy (SEM, SIGMA 300 VP, Zeiss) at low vacuum, without sputtering.

2.2 | Leaf Anatomy

For optical microscopy (OM) and transmission electron microscopy (TEM) examination, lettuce leaves were cut into 4 mm^2 pieces (20 leaf sections were fixed by collecting two pieces per leaf and a total of 10 plants sampled) and fixed in 2.5% glutaraldehyde and 4% paraformaldehyde (both from Electron Microscopy Sciences) for 3 h at 4°C. Samples were rinsed in cold phosphate buffer (7.2 pH) four times for 6 h and were kept at 4°C for 12 h. Leaf pieces were postfixed in a 1:1 aqueous solution of osmium tetroxide (2%, TAAB Laboratories) and potassium ferrocyanide (3%, Sigma-Aldrich, Germany) for 1.5 h. They were rinsed in distilled water (×3), dehydrated in an acetone series (30%, 50%, 70%, 80%, 90%, 95% and 100%; ×2, 15 min for each concentration), and embedded in acetone-Spurr's resin (TAAB Laboratories) mixtures (v:v 3:1 for 2 h, 1:1 for 2 h, 1:3 for 3 h) and finally in pure resin, keeping samples at room temperature. After 12 h, lettuce leaf sections were placed in blocks filled with pure resin before incubation at 70°C for 3 days until complete resin polymerisation. Ultra-thin sections (obtained with a Leica Ultracut E) were cut, mounted on nickel grids and poststained with Reynolds lead citrate (EMS) for 5 min before microscopic observation. Five leaf cross-sections were observed with a TEM Jeol 1010 (Jeol Ltd., at 80 kV) equipped with a CCD Megaview camera (National Electron Microscopy Centre, Complutense University of Madrid, Spain). On the other hand, for leaf OM analysis, semi-thin cross-sections were cut, mounted in microscope slides and stained with Toluidine Blue before observation with an epifluorescence microscope (Axioplan-2, Zeiss, $N = 5$).

2.3 | Contact Angle Measurements

Pseudo-equilibrium and dynamic contact angles (θ) were determined for both leaf sides of lettuce. First, pseudo-equilibrium contact angles were estimated by rapidly depositing 2 μL drops of distilled water, glycerol (ReagentPlus, 99%, Sigma-Aldrich) and diiodomethane (ReagentPlus, 99%, Sigma-Aldrich) onto the adaxial and abaxial leaf surfaces with a 1 mL syringe having a 0.5 mm diametre needle ($N = 30$ for each liquid, with six drops applied to the upper or lower side of the leaf lamina of fully expanded, healthy leaves of five different plants). Second, dynamic contact angles (advancing [θ_{adv}] and receding [θ_{rec}]) and contact angle hysteresis ($\Delta\theta_{hys}$) were also measured with distilled water drops ($N = 10$; two drops of water were applied to the lower or upper leaf side of five plants). Measurements were carried out at room temperature (21°C–23°C) with a Drop Shape Analysis System (DSA 100, Krüss Scientific), making sure leaves were turgid at the time of sampling. The tangent method was used to calculate the contact angle values from side-view images of drops.

The total surface free energy (γ), its components (i.e., Lifshitz–van der Waals [γ_s^{LW}] and acid–base [γ_s^{AB}, γ_s^+ and γ_s^-]), the degree of polarity (%) and solubility parametre (δ) of lettuce leaf surfaces were estimated by considering the following surface tension values of three liquids: $\gamma_l = 72.80\ mJ\ m^{-2}$, $\gamma_l^{LW} = 21.80\ mJ\ m^{-2}$, $\gamma_l^+ = \gamma_l^- = 25.50\ mJ\ m^{-2}$ for water, $\gamma_l = 63.70\ mJ\ m^{-2}$, $\gamma_l^{LW} = 33.63\ mJ\ m^{-2}$, $\gamma_l^+ = 8.41\ mJ\ m^{-2}$, $\gamma_l^- = 31.16\ mJ\ m^{-2}$ for glycerol and $\gamma_l = \gamma_l^{LW} = 50.80\ mJ\ m^{-2}$, $\gamma_l^+ = 0.56\ mJ\ m^{-2}$, $\gamma_l^- = 0\ mJ\ m^{-2}$ for diiodomethane (Fernández and Khayet 2015).

2.4 | Atomic Force Microscopy

The nano-scale topography and wettability of fresh and CPD lettuce leaf surfaces (analysing three zones of five different leaf sections collected from five different plants) were estimated by Dynamic Atomic Force Microscopy (Nanotec Electronica) equipped with a phase-locked loop (PLL) board (bandwidth ~2 kHz). Measurements were performed in Amplitude Modulation Dynamic AFM mode (AM-DAFM), using amplitude as the primary feedback signal. A relatively large free oscillation amplitude ($a_{free} \approx 25$ nm) and low amplitude set-point ($a_{set}/a_{free} \approx 0.9–0.8$) ensured tip-sample interaction remained within the attractive, noncontact regime. Silicon tips (Olympus

13993054, 2025, 5, Downloaded from https://onlinelibrary.wiley.com/doi/10.1111/ppl.70580 by Victoria Fernandez - Spanish Cochrane National Provision (Ministerio de Sanidad) , Wiley Online Library on [17/10/2025]. See the Terms and Conditions (https://onlinelibrary.wiley.com/terms-and-conditions) on Wiley Online Library for rules of use; OA articles are governed by the applicable Creative Commons License

TABLE 1 | Equilibrium contact angles (θ_0) for drops of water, glycerol and diiodomethane with the upper and lower sides of Romaine lettuce leaves. For water, advancing (θ_{adv}), receding (θ_{rec}) contact angles and contact angle hysteresis ($\Delta\theta_{hys}$) are provided. Data are means ± standard deviations (SD; $N = 30$ for equilibrium contact angles and $N = 10$ for dynamic contact angles). For the same liquid, letters indicate homogenous groups according to Tukey's HSD (honestly significant difference) test ($p < 0.05$).

	Surface	Contact angles (°)			
Liquid	**Leaf side**	**Equilibrium (θ_0)**	**Advancing (θ_{adv})**	**Receding (θ_{rec})**	**Hysteresis ($\Delta\theta_{hys}$)**
Water	Adaxial	75.1 ± 7.4 a	81.8 ± 4.9 a	29.5 ± 4.2 a	51.8 ± 5.4 a
	Abaxial	64.3 ± 8.3 a	73.0 ± 7.8 a	22.4 ± 5.1a	50.8 ± 5.0 a
Glycerol	Adaxial	56.5 ± 6.5 a			
	Abaxial	58.1 ± 5.8 a			
Diiodomethane	Adaxial	62.4 ± 5.1 a			
	Abaxial	57.5 ± 6.6 a			

AC240TS) with a nominal force constant of 2 N/m and tip apex radius of 15 nm were used. The height range was limited by the piezo actuator, which has a maximum vertical scan range of 10 μm, meaning that certain surface areas could exceed the measurable height.

Fresh lettuce leaves were marked and photographed at 5× optical zoom (Figure 4A), enabling AFM images (Figure 4C,D) to be directly correlated with SEM images (Figure 4B); the yellow square in the SEM image indicates the AFM scanning region. Samples were mounted on holders compatible with both AFM and SEM platforms. Topography *z(x,y)* and wettability *w(x,y)* images were acquired simultaneously using dual feedback loops. The first loop controlled the amplitude for topography acquisition, while the second PLL controlled the tip-sample resonance frequency shift, $\delta\nu(x,y) = \nu(x,y) - \nu_0$ (where ν_0 is the free resonance frequency), to generate the wettability map. This $\delta\nu(x,y)$ signal is sensitive to the chemical composition of the surface (Almonte et al. 2022; Fernández et al. 2024).

The wettability channel *w(x,y)* reflects the formation and rupture of the liquid neck between the tip and the leaf surface under room conditions (25°C, 50% relative humidity), as previously described (Colchero et al. 1998; Palacios-Lidón et al. 2009). These maps allow local characterisation of hydrophilic and hydrophobic regions (Figure 4F,H). For precise spatial correlation, a 3D overlay was created by superimposing *w(x,y)* onto *z(x,y)* (Figure S2), where hydrophilic zones (stronger capillary interaction) appear in blue, and hydrophobic zones (weaker interaction) appear in red/yellow. Image processing and analysis were performed using WSxM software (Horcas et al. 2007).

2.5 | Fourier Transform Infrared (FTIR) and Confocal Raman Spectroscopy

Attenuated Total Reflectance (ATR)–FTIR spectroscopy analyses of fresh and CPD lettuce leaf sections (spectra of three sections of three different fully expanded, healthy leaves from three different plants) were carried out with a FTIR spectrometre (Nicolet iS50, Thermo Fisher Scientific). Measurements were made in absorbance mode, in the 4000–400 cm^{-1} spectral range, collecting the background before each leaf sample analysis.

Fresh lettuce leaves (generally, three to five zones of five sections collected from five different leaves and plants) were also examined by confocal Raman microscopy (XPlora, Horiba MTB equipped with 785, 638 and 532 nm excitation lasers). The laser power was controlled with a 1% filter, resulting in an output power of 110 W for 532 nm excitation and 706 W for 785 nm excitation. Measurements were conducted using a 50× (long working distance, N.A. 0.5) objective, giving a lateral spatial resolution of circa 2 μm. Additional spectra (not shown) were obtained with a 100× objective (N. A. 0.90), with similar results at the cost of longer integration times. 1200 g/mm (600 g/mm) gratings were used for high (low)-resolution spectra. To obtain Raman maps, the acquisition parametres were optimised to achieve the best signal-to-noise ratio, while minimising laser exposure time and intensity to prevent sample dehydration and surface defocusing. Optimal conditions for an 11 × 11 points scan matrix (121 points, 2 μm step) were established with an exposure time of 1 s and a single accumulation using low-resolution gratings. Best results were recorded when immersing leaf samples in water during measurement.

3 | Results

3.1 | Lettuce Leaf Wettability

The wettability of lettuce was assessed by measuring contact angles of water, glycerol and diiodomethane (Table 1). The upper and lower leaf sides of lettuce are wettable ($\theta < 90°$) for all tested liquids. In general, pseudo-equilibrium contact angles were lower for the abaxial surface, except for glycerol, where values were practically similar for both surfaces. In any case, for the same liquid, no statistically significant differences were recorded between leaf sides. Both surfaces had a major and a similar degree of adherence of water drops as derived from the 51° to 52° contact angle hysteresis values recorded.

The surface free energy and related parametres of the upper and lower sides of Romaine lettuce leaves were estimated according to the 3-Liquids method (Table 2). In general, for both leaf sides, the surface free component and total surface free energy values were within a similar range and had a high polarity of 24%–25%. Compared to the abaxial (upper) surface, the abaxial leaf side

13993054, 2025, 5, Downloaded from https://onlinelibrary.wiley.com/doi/10.1111/ppl.70580 by Victoria Fernandez - Spanish Cochrane National Provision (Ministerio de Sanidad) , Wiley Online Library on [17/10/2025]. See the Terms and Conditions (https://onlinelibrary.wiley.com/terms-and-conditions) on Wiley Online Library for rules of use; OA articles are governed by the applicable Creative Commons License

had a slightly higher γ_s and solubility parametre (δ) value, which can be associated with the higher contribution of the negative surface free energy component (γ^-). The low contact angles with liquids having a significant nondispersive component (i.e., water and glycerol) and a high degree of polarity ($\gamma^{AB}\ \gamma_s^{-1}$) rendered this surface suitable for evaluating the occurrence of nano-hydrophilic areas in its cuticle; more detailed characterisation trials were performed as described below.

3.2 | Leaf Surface Structure

The morphology of fresh (immediately observed with no treatment after tissue sectioning) and critical point dried (CPD) Romaine lettuce leaf sections was first analysed by SEM, as shown in Figure 1. Both leaf surfaces are similar to some extent. They have densities of 105 ± 27 (abaxial) and 126 ± 32 (adaxial) stomata per mm^2. Furthermore, adaxial and abaxial side stomata (Figure 1B,F) and the surrounding pavement cells are morphologically similar. No major surface differences were detected between fresh and CPD lettuce samples in terms of morphological changes.

In Figure 2, the structure of the lettuce leaf after tissue staining with toluidine blue (Figure 2A) or metals (Figure 2B–F) is shown. Epidermal cells are the interface with the surrounding atmosphere and mostly include rather rectangular, big pavement cells (Figure 2A), with scattered pairs of guard cells forming a stoma both on the adaxial and abaxial leaf sides. When examining the cell wall of stomata by TEM (Figure 2B–D), stomatal ledges having a heterogeneous deposition of lipids with a reticulate pattern can be observed as a material generating a concave, protruding structure over the pore, resembling a volcano. Cell wall pegs also covered with a heterogeneous, reticulate cuticle occur at the base of guard cells, close to the stomatal chamber (Figure 2D). In general, the cuticle of stomatal ledges and pegs (Figure 2C,D) is reticulate and belongs to Type 4, according to Holloway's classification (Holloway 1982; Jeffree 2006). However, changes in guard cell cuticle thickness and ultra-structure were detected from the ledge toward the end of the guard cells (see Figure 2C,E). Nano-areas of cell wall polysaccharides can actually be distinguished in guard cell parts located approximately $> 5\,\mu m$ away from the ledge toward the neighbouring epidermal cell (Figure 2E). By contrast, adaxial and abaxial pavement cells have a thicker and amorphous Type 6 cuticle (Figure 2F) (Holloway 1982). The heterogeneous cuticular ultra-structure of lettuce leaf epidermal cells as observed by TEM can be associated with variable chemical composition and structural arrangement of surface chemical constituents, as further analysed by AFM microscopy.

3.3 | Raman and FTIR Spectroscopy

Adaxial and abaxial surfaces of fresh and CPD Romaine lettuce leaves were qualitatively analysed by FTIR (Figure 3A). To facilitate comparisons, stacked average FTIR spectra (Figure 3A) were used to visualise differences across replicates and treatments. The presence of the same characteristic peaks, as well as the absence of shift, can be observed in all samples and their replicates.

The average FTIR spectra of the adaxial and abaxial surfaces of fresh and CPD Romaine lettuce leaf samples had similar

TABLE 2 | Total surface free energy (γ). Lifshitz–van der Waals component (γ^{LW}). Acid–base component (γ^{AB}) with the contribution of electron donor (γ^-) and electron acceptor (γ^+) interactions, total surface free energy (γ_s) and polarity ($\gamma^{AB}\ \gamma_s^{-1}$) of adaxial and abaxial leaf surfaces of Romaine lettuce.

Leaf side	γ^{LW} (mJ m^{-2})	γ^- (mJ m^{-2})	γ^+ (mJ m^{-2})	γ^{AB} (mJ m^{-2})	γ_s (mJ m^{-2})	Polarity (%)	δ (mJ$^{1/2}$ m$^{-3/2}$)
Adaxial	27.2	5.3	3.8	8.9	36.1	24.7	18.3
Abaxial	30.0	16.8	1.4	9.6	39.6	24.2	19.6

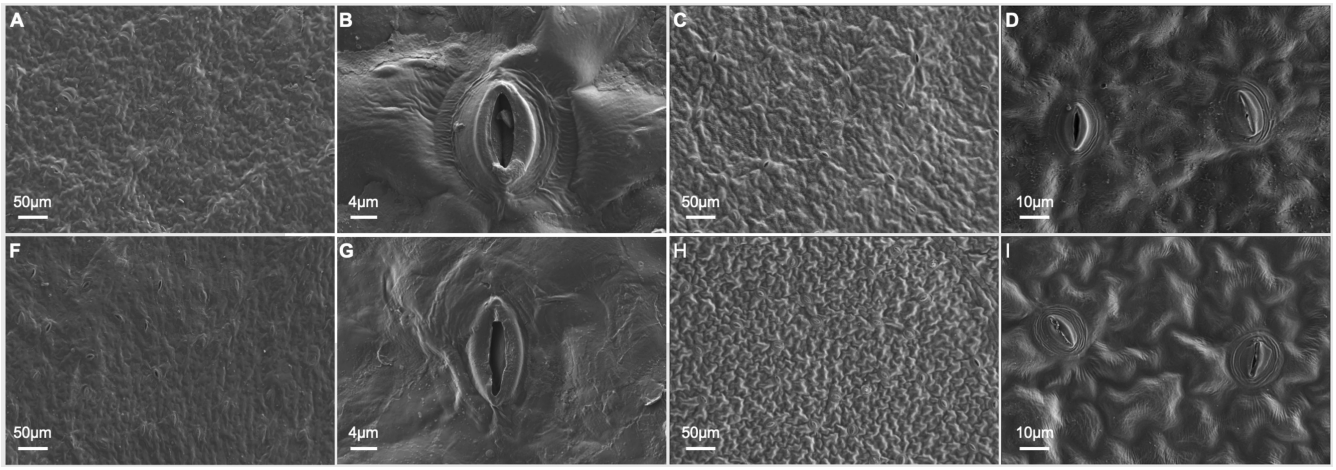

FIGURE 1 | Adaxial (A–D) and abaxial (F–I) lettuce leaf surfaces observed by SEM. Micrographs correspond to fresh (A, B, F and G) and CPD (C, D, H and I) leaf tissues.

13993054, 2025, 5, Downloaded from https://onlinelibrary.wiley.com/doi/10.1111/ppl.70580 by Victoria Fernandez - Spanish Cochrane National Provision (Ministerio de Sanidad) , Wiley Online Library on [17/10/2025]. See the Terms and Conditions (https://onlinelibrary.wiley.com/terms-and-conditions) on Wiley Online Library for rules of use; OA articles are governed by the applicable Creative Commons License

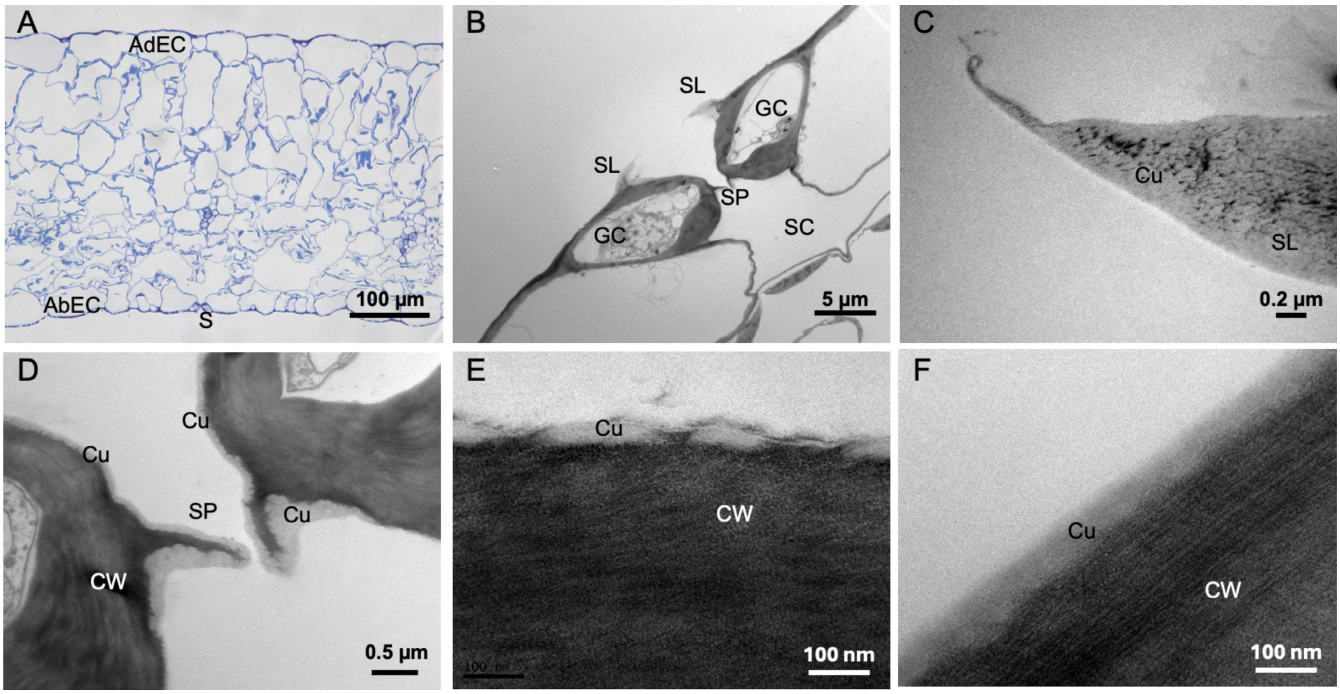

FIGURE 2 | Cross-sections of Romaine lettuce leaves and epidermal cells observed by optical microscopy (A) or TEM (B–F). (A) Leaf general anatomy, (B) detail of a stoma and its guard cells protecting the substomatal cavity, (C) detail of the cuticle of a stomatal ledge, (D) cuticle of stomatal pegs toward the top of the substomatal cavity, (E) cuticle of the central part of a guard cell toward the neighbouring epidermal cell showing an irregular cuticle deposition and cell wall nano-areas as leaf-air interface material and (F) example of an adaxial or abaxial pavement cell cuticle cells having an amorphous ultrastructure. AbEC, abaxial epidermal cell; AdEC, adaxial epidermal cell; Cu, cuticle; CW, cell wall; GC, guard cell; SC, substomatal cavity; SL, stomatal ledge; SP, stomatal peg.

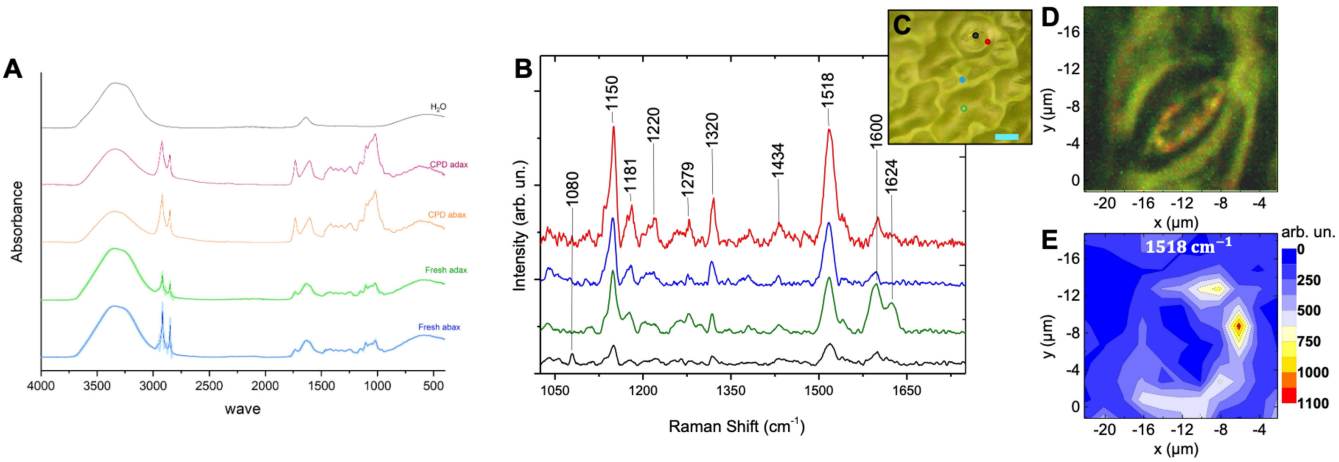

FIGURE 3 | FTIR and Raman spectroscopy spectra of lettuce leaves. (A) FTIR spectra of adaxial and abaxial fresh and CPD leaf surfaces. Each spectrum shows the mean signal (solid line) and standard deviation (shaded area). (B) High-resolution Raman spectra of Roman lettuce (adaxial side) obtained from four points of interest, as indicated in the optical micrograph (C). Optical image, the scale bar corresponds to 10 µm. Spectra were measured at the stomatal ledge (red), stomatal cavity (black), epidermal cell (green) and cell wall (blue) with 785 nm excitation. (D) Optical micrograph of the stoma corresponding to the area selected for Raman imaging obtained with 532 nm excitation. Univariate analysis (band integration) has been used at the peak 1518 cm^{-1} in (E).

characteristic peaks (Figure 3A,B). However, a remarkable decrease in the intensity of certain peaks is observed when comparing fresh versus CPD samples, primarily affecting O–H-related vibrational modes. This reduction is attributed to differences in water content between the two samples. The removal of water in CPD leaves improved the observation of specific chemical compound peaks. Actually, none of the peaks corresponding to functional groups detected in fresh lettuce leaf surfaces disappeared in CPD samples, indicating that this treatment did not induce significant chemical alterations. Furthermore, CPD preserved surface topography, ensuring the structural integrity of the tissues for subsequent analyses (Figure 3A).

13993054, 2025, 5, Downloaded from https://onlinelibrary.wiley.com/doi/10.1111/ppl.70580 by Victoria Fernandez - Spanish Cochrane National Provision (Ministerio de Sanidad) , Wiley Online Library on [17/10/2025]. See the Terms and Conditions (https://onlinelibrary.wiley.com/terms-and-conditions) on Wiley Online Library for rules of use; OA articles are governed by the applicable Creative Commons License

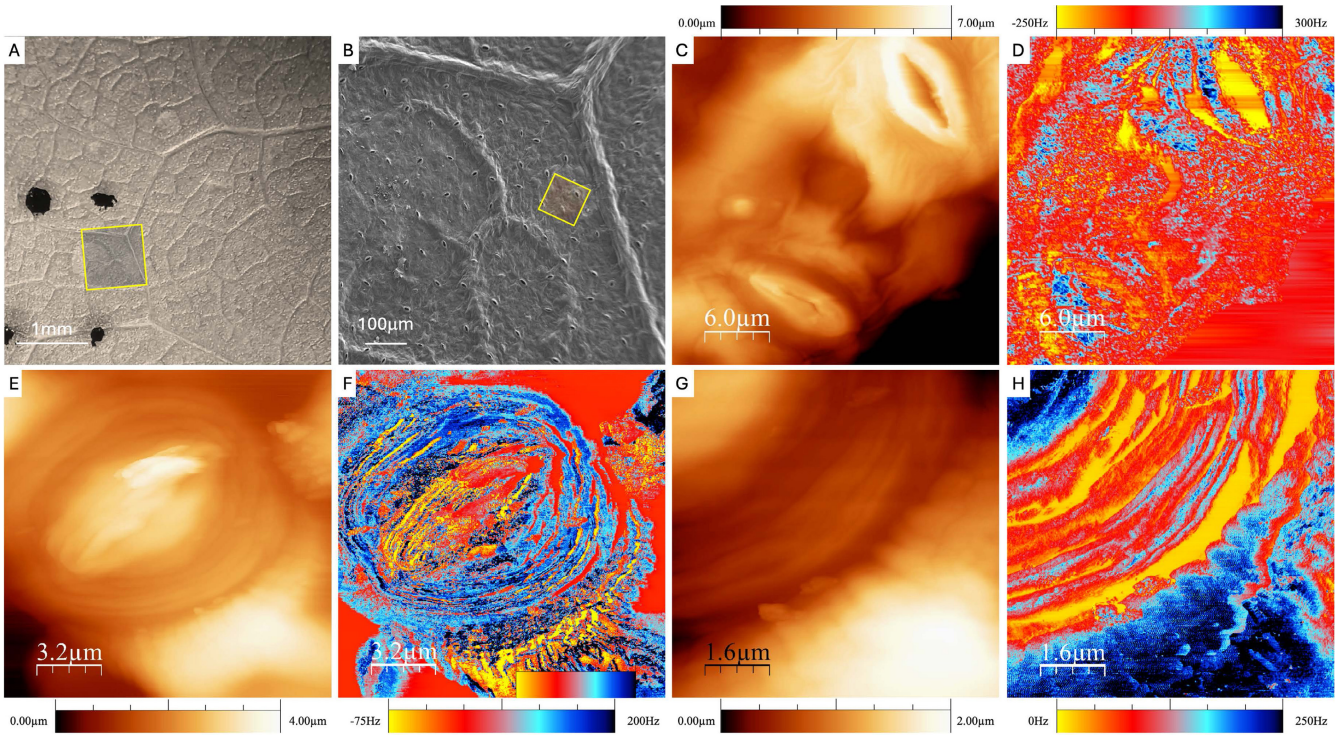

FIGURE 4 | Correlation between (A) optical, (B) SEM, (C) AFM topography and (D) wettability images of the same region of a fresh Romaine lettuce leaf. High-resolution AFM topography (E) and wettability (F) images of a stomatal pore of CPD leaf samples. (G) Close-up of the stomatal region with cuticular folds at the base of the cuticular ledges, and (H) corresponding wettability image, illustrating changes in hydrophilicity along the folds. The wettability maps are expressed in arbitrary units (Hz).

The broad band at 3650–3000 cm^{-1} is characteristic of hydroxyl (–OH) groups, due to hydrogen-bond interactions. The compounds related to this band primarily include cuticular polysaccharides, which are rich in –OH groups, but also cutin/cutan polymers (Heredia-Guerrero et al. 2014). In addition, a broad and low-intensity band at 583 cm^{-1} is observed, which can be attributed to out-of-plane bending due to –OH groups. All the characteristic peaks present in both leaf spectra exhibit similar intensity and sharpness. High-intensity peaks between 2918 and 2850 cm^{-1} correspond to symmetric and asymmetric C–H stretching of $–CH_2–$ groups in the aliphatic chains of cutin/cutan and waxes (Heredia-Guerrero et al. 2014). Accompanying bending vibrations appear around 1463 ($–CH_2–$) and 1372 cm^{-1} ($–CH_3$). A weak 720 cm^{-1} peak indicative of long aliphatic chains is observed in all the samples. However, this peak is poorly visible due to the higher intensity of out-of-plane bending of –OH groups.

A prominent band at 1735 cm^{-1} linked to C=O stretching vibration of ester and carboxylate groups can be associated with cutin polymer but may also arise from polysaccharide-derived ester linkages (Heredia-Guerrero et al. 2014). As shown by Pesquet et al. (2013), the presence or absence of specific FTIR bands, such as those linked to lignin (e.g., 1510 and 1595 cm^{-1}), can vary significantly depending on the state of the sample and the presence of specific monomers (Heredia-Guerrero et al. 2014). Although the current study does not involve lignified tissues or vascular cell types like tracheary elements, the interpretation of shared peaks is also pertinent. Nevertheless, the observed spectral differences between fresh and CPD-treated samples remain consistent across replicates and support the qualitative interpretation of lettuce leaf surface components. Carbon–O–C stretching vibrations appear at 1100 (symmetric) and 1147 cm^{-1} (asymmetric). Peaks within 800–500 cm^{-1} include a band at 833 cm^{-1}, attributed to out-of-plane C–H bending in aromatic compounds like phenolics and flavonoids. Additionally, a broad band at 1600–1630 cm^{-1} is due to C=C stretching in phenolic compounds (Heredia-Guerrero et al. 2014).

Raman spectra (785 nm excitation) were recorded at four points on the adaxial surface of fresh lettuce leaves (Figure 3B). In the spectra shown, the optimised Raman mapping setup employed a 50× objective with a numerical aperture (NA) of 0.5 and a medium confocal aperture (300 µm), using 532 nm excitation. Under these conditions, the axial resolution is approximately 3 µm. During the scan, the leaf surface may shift by up to 2 µm due to dehydration. The combination of these factors leads to an estimated uncertainty of ±5 µm in focus determination. Additionally, the height variation across the mapped stoma is on the order of 5 µm. Therefore, in our case, the accuracy of the z-stage positioning is insufficient to justify including a colour scale in Figure 3D,E. The Raman map shown in Figure 3 is representative of the results gathered for three different areas of the leaf section analyzed and for other leaves measured ($N = 5$). Nonetheless, two more Raman maps are provided as Supporting Information. We also evaluated the correlation between the intensities of P1, P2 and P3 peaks with the P4 peak, as labelled in the spectra.

Prominent bands at 1600 and 1624 cm^{-1}, particularly intense in stomatal cavities or underneath epidermal pavement cells

13993054, 2025, 5, Downloaded from https://onlinelibrary.wiley.com/doi/10.1111/ppl.70580 by Victoria Fernandez - Spanish Cochrane National Provision (Ministerio de Sanidad) , Wiley Online Library on [17/10/2025]. See the Terms and Conditions (https://onlinelibrary.wiley.com/terms-and-conditions) on Wiley Online Library for rules of use; OA articles are governed by the applicable Creative Commons License

(green spectrum), were attributed to aromatic ring stretching in phenolic compounds (Sasani et al. 2021; Blaschek et al. 2023). Consistent with FTIR findings, these bands can be attributed to the occurrence of phenolic compounds (Gupta et al. 2020). Additionally, less intense peaks were identified at 1181 cm^{-1} (C–O–H stretching adjacent to an aromatic ring, CH vibrations), 1220 and 1279 cm^{-1} (C–C–H bending), 1320 cm^{-1} (–CH_2– bending) and 1434 cm^{-1} (–CH_2– stretching), consistent with findings from previous studies (Farber et al. 2019). A very weak peak at 1080 cm^{-1} was detected exclusively in stomatal cavities (Figure 3B,C in black) and to a lesser extent, in stomatal ledges. This peak likely arises from multiple functional groups, including ν(C–O), ν(C–C) or δ(C–O–H) vibrations (Heredia-Guerrero et al. 2014). Besides these bands, two prominent peaks were observed at 1150 (ν_3) and 1518 cm^{-1} (ν_1) (Figure 3E), corresponding to the strongest Raman bands which may be attributed to carotenoids (Gupta et al. 2020; Schulz et al. 2005; De Gelder et al. 2007).

3.4 | Atomic Force Microscopy

To correlate the local adhesion force with the local wetting parametre, AFM measurements were conducted in dynamic mode. The oscillation amplitude served as a feedback signal for topographic imaging, and a low amplitude reduction was applied to minimise tip–sample interactions, ensuring operation within the attractive regime. The tip–sample resonance frequency shift was monitored using the PLL system and recorded as an additional data channel, providing complementary information on the sample's chemical composition. Wettability measurements derived from frequency shifts (Figure 4D,F,G) reveal regions with a high probability for liquid neck formation, indicative of enhanced local surface interactions without direct mechanical contact. These wettability maps, expressed in arbitrary units (Hz)', offer a visualisation of hydrophilic and hydrophobic domains across the leaf surface; see Supporting Information (Almonte et al. 2022). Figure 4C shows a topographical average roughness (rms) of 1.30, while Figure 4D represents the wettability, *w(x,y)*, with a resolution of 118/pixel. Collecting the image at this resolution generates average values, providing a first approximation to the wettability image. This wettability image provides a detailed visualisation of variable liquid neck interactions across different regions of the sample, with stronger liquid neck interactions in certain areas, depicted by bluish hues. Higher-resolution data were obtained for CPD-treated lettuce (Figure 4E,F), with Figure 4F showing the wetting image at 16 nm/pixel. This image provides a broader view of the study area, with Figure 4G,H offering an enlarged and more detailed perspective of the stomatal folds, at a resolution of 8 nm/pixel, which essentially corresponds to the experimental limit of our technique. In these latter two images, the cuticular folds of stomata were analysed, because they exhibited variable interactions with liquid necks compared to other epidermal cells, indicating a higher attraction of hydrophilic regions, as indicated by the blue colouration. In such stomatal cuticular folds, a variety of hydrophilic/hydrophobic zones can be observed. These heterogeneous areas in stomata occurred in the adaxial and abaxial leaf sides and were similar for fresh lettuce and CPD samples. Furthermore, AFM imaging revealed significant height variations at the micro- and nano-scale levels, even within regions that were closely spaced, with separations as small as a few nanometres.

4 | Discussion

In this study and based on previous investigations performed with leafy green vegetables, we selected a wettable Romaine lettuce variety with a high degree of leaf surface polarity for testing whether leaves may be chemically heterogeneous at the nanoscale and if the existing hydrophilic areas were epidermal cell-specific. By using several microscopic and analytical techniques, we gained evidence that our parting hypotheses were verified. In two previous studies, we showed the occurrence of few hydrophilic nano-zones in poorly wettable rose petals having the rose petal effect (i.e., very high contact angles and water drop adhesion) (Almonte et al. 2022) and a higher frequency of them detected in the trichomes on olive leaves (Fernández et al. 2024), which are at the unwettable threshold for the abaxial side (i.e., 90°). Hence, based on the existing literature on the wettability of leafy green vegetables (Lu et al. 2015; Ku et al. 2020; Truschi et al. 2023), we selected lettuce as a potential model for a plant surface having a higher frequency of hydrophilic nano-areas in its foliage. The wettable lettuce variety analysed was actually found to have a high frequency of hydrophilic nano-zones chiefly in adaxial and abaxial leaf stomatal areas. In the paragraphs below, the significance of our results will be gradually discussed, emphasising the potential role of hydrophilic nano-zones in the cuticle in functional and eco-physiological terms, which should be further analysed in future investigations.

Plant surfaces have major importance. New AFM techniques (Almonte et al. 2022) enable mapping for the first time the nanoscale distribution of hydrophilic and hydrophobic compounds, which multiplies the complexity of current views on cuticle composition and structure in relation to its potential functionality. However, the link between macroscopic wettability (i.e., as determined with water contact angles) of plant surfaces and their composition and chemical localisation still remains unclear, and traditional approaches considering the cuticle a continuous, lipid layer (e.g., Suh et al. 2005) may be over-simplistic, at least for some epidermal cell areas, organs and species.

For attempting to characterise the occurrence of hydrophilic areas in plant surfaces at the nano-scale, we analysed the samples by AFM in true noncontact mode, in which the cantilever tip does not physically contact the sample surface (Almonte et al. 2022; Fernández et al. 2024). This approach does not alter the morphology and chemical composition of the lettuce leaf cuticle. By contrast, the AFM force mapping technique (peak force or pinpoint, for example), used by, for example, Ménard et al. (2022), involves direct tip-sample contact, allowing for relative quantification of mechanical properties such as stiffness and adhesion force attributes influenced by processes like lignification.

Lettuce is an important horticultural commodity that is quite perishable and susceptible to pest and disease contamination (Peng and Simko 2023). Several investigations and technical reports (Esseili et al. 2012; Lu et al. 2015) referred to human, food-borne illnesses associated with the consumption of leafy

13993054, 2025, 5, Downloaded from https://onlinelibrary.wiley.com/doi/10.1111/ppl.70580 by Victoria Fernandez - Spanish Cochrane National Provision (Ministerio de Sanidad) , Wiley Online Library on [17/10/2025]. See the Terms and Conditions (https://onlinelibrary.wiley.com/terms-and-conditions) on Wiley Online Library for rules of use; OA articles are governed by the applicable Creative Commons License

vegetables, and some studies chiefly related their contamination susceptibility to leaf wettability and stomatal traits (Ku et al. 2020; Truschi et al. 2023; Dong et al. 2024).

Surface chemical composition and structure affect the barrier properties of leaves and other aerial plant organs, for example, favouring or impeding foliar water absorption (Schreel et al. 2020; Fernández et al. 2021; Liu et al. 2023; Losso et al. 2023) or by affecting the rate of residual transpiration (Isaacson et al. 2009). The characterisation of leaf surface wettability and surface free energy is useful for evaluating the combined effect of surface chemical composition and roughness and provides information on potential surface interactions with water and surface-deposited matter of ecological and agro-forestry interest (Smith and McClean 1989; Brewer et al. 1991; Koch et al. 2008; Rosado and Holder 2013; Fernández et al. 2021). The contact angle values measured for the three liquids of different degrees of polarity/apolarity were below 90°, indicating that such surfaces are wettable. In addition, lettuce leaf surfaces had a total surface free energy of approximately 36–40 $mJ\,m^{-2}$ and a high degree of polarity (24%). The contact angles and surface free energy values estimated for Romaine lettuce surfaces are similar to the adaxial leaf side of Arbequina olive leaves (Fernández et al. 2024) or some corn variety leaves (Revilla et al. 2016; Henningsen et al. 2023). Such surfaces are wettable and have relatively low roughness compared with plant surfaces having cuticular folds, hydrophobic trichomes or nano-structured epicuticular waxes (Koch et al. 2008; Fernández et al. 2021). Nonetheless, AFM images revealed a high average roughness of 700 nm rms over a $10 \times 0\,\mu m$ area, indicating that a substantial amount of leaf surface may be covered with liquid droplets deposited onto it. The relatively low roughness of Romaine lettuce leaves compared with other leafy greens, such as cabbage or mustard (Lu et al. 2015), can facilitate the growth of microorganisms (Chiu et al. 2020; Truschi et al. 2023), highlighting the importance of leaf surface features for assessing potential interactions with surface-deposited matter.

Working with 'Two Star' lettuce variety, Ku et al. (2020) evaluated the leaf wax composition, wettability and degree of *Salmonella* spp. attachment to surfaces of leaves at different ages and positions. Contrary to our wettable 'Turbina' lettuce, in which we could not identify a distinct layer of epicuticular waxes, Ku et al. (2020) observed crystalised epicuticular waxes and higher water contact angles. In general, wettable leafy greens, such as lettuce, may have lower amounts of epicuticular waxes (e.g., 5–10 $\mu g\,cm^{-2}$ soluble cuticular lipids) compared to some cabbage or mustard varieties (70–80 $\mu g\,cm^{-2}$ soluble cuticular lipids) (Lu et al. 2015; Palma-Salgado et al. 2020). Alike in the rose petals of 'Lois Lane' cultivar (Almonte et al. 2022), there was a lack of a distinct epicuticular wax layer in the 'Turbina' Romaine lettuce leaves analysed, which implies that measurements were largely carried out on the cuticle surface as observed in TEM and SEM images (Figures 1 and 2). By AFM, we were able to assess the difference in wettability of stomatal edges compared to the base of guard cells. This is related to the greater probability of adherence of certain zones due to the formation of liquid necks, which can be associated with areas of increased hydrophilicity.

Lettuce leaf cuticles are rather thin (< 100 nm) compared to other species (Jeffree 2006). The cuticular ultra-structure of epidermal cells is rather amorphous and can be assigned to Type 6 (Holloway 1982). Nonetheless, depending on the epidermal cell area analysed with special regard to stomata, the cuticle may have variable thickness and ultra-structure as derived from the occurrence of electron-dense and electron-lucent areas (e.g., Figure 2F).

The surface of many plant and biological materials is difficult to characterise owing to its rapid perishability and loss of shape due to dehydration and cell collapse. For this reason, techniques such as critical point or chemical drying have been introduced for surface analysis (Bhattacharya et al. 2020). Thereby, we also carried out measurements with CPD lettuce pieces which were chemically similar to the fresh ones, as demonstrated by FTIR. Based on our AFM measurements, we observed no major differences in the topography and wettability of CPD versus fresh lettuce leaf samples (Figure 4).

Lettuce leaf stomatal pores are encrypted by a cuticle forming a 'volcano-like' structure, as reported for other plant species (e.g., Jordan et al. 2008; Roth-Nebelsick et al. 2013). The upper part of the crypt has thin, reticulate, cuticular ultra-structure (Type 4, Holloway 1982). At the base of the stomatal crypt, which approximately begins to form in the middle of the guard cell toward the pore, we observed cuticular folds, which will also influence surface wettability. The nano-scale heterogeneity of the cuticle-forming stomatal crypts, as depicted in our AFM images, supports the occurrence of hydrophilic material in stomatal regions, as also observed in guard-cell TEM cross-sections. Altogether, our microscopy images provide clear evidence for the nano-scale, chemical heterogeneity of lettuce leaves, which have a higher density of hydrophilic nano-areas chiefly in stomatal surfaces, compared to olive leaf trichomes and rose petals (Almonte et al. 2022; Fernández et al. 2024). Alike in olive leaves (Fernández et al. 2024), the occurrence of hydrophilic nano-areas on lettuce leaf surface will also contribute to the high water wettability and drop adhesion of such plant materials.

The lack of an identifiable epicuticular wax layer in combination with the occurrence of hydrophobic-hydrophilic material at the nano-scale chiefly in stomatal areas is reflected in the wettability maps obtained by AFM. The large chemical variability of these surfaces suggests distinct hydrophilic-hydrophobic material regions. These findings are supported by the heterogeneous cuticular patterns observed in lettuce leaf TEM cross-sections, which likely indicate the presence of cell wall polysaccharides. The detection of hydrophilic nano-zones especially in lettuce leaf stomatal pores suggests that they may be preferential areas for microorganism attachment and proliferation. Esseili et al. (2012) found that Norovirus binds to exposed cell wall polysaccharides, with a preference for older leaves and leaf lamina zones. Thereby, it is likely that pathogens with an affinity for cell wall polysaccharides will adhere and proliferate in the hydrophilic nano-areas detected by AFM and TEM, rendering lettuce leaves more susceptible to pathogen contamination. These hydrophilic nano-areas, mainly occurring in stomata, will also provide a more favourable environment for microbial growth due to the high moisture of stomatal pores (Roth-Nebelsick et al. 2013). High rates of leaf water loss during storage and commercialisation can reduce the shelf life and quality of lettuce. Hence, understanding the distribution and properties of

13993054, 2025, 5, Downloaded from https://onlinelibrary.wiley.com/doi/10.1111/ppl.70580 by Victoria Fernandez - Spanish Cochrane National Provision (Ministerio de Sanidad) , Wiley Online Library on [17/10/2025]. See the Terms and Conditions (https://onlinelibrary.wiley.com/terms-and-conditions) on Wiley Online Library for rules of use; OA articles are governed by the applicable Creative Commons License

nano-hydrophilic areas potentially occurring in the surface of leaves and aerial plant organs will be crucial for developing strategies to enhance the marketability and storability of horticultural commodities.

Leaf surface chemical heterogeneity and epidermal cell-specific cuticular changes can also have major eco-physiological implications, at least in terms of variable surface interactions, transport phenomena and mechanical properties, which should be further elucidated. For example, the presence of hydrophilic nano-areas in the surface stomata or other epidermal cells may increase the residual transpiration of plant organs and affect current water and gas transport models across plant surfaces. They may also contribute to foliar water uptake (Schreel et al. 2020; Losso et al. 2023; Liu et al. 2023) and to water condensation mechanisms (Fernández et al. 2024); this should be characterised in future eco-physiological studies.

5 | Conclusions

The properties of 'Turbina' Romaine lettuce leaves have been analysed with a battery of complementary techniques with spatial resolutions that range from nano-metres to milli-metres. Surfaces were found to be wettable and chemically heterogeneous at the nano-scale, especially regarding stomata. Nano-hydrophilic areas have been localised in the abaxial and adaxial leaf surfaces with a focus on stomata. Future studies should elucidate their functional significance. The occurrence of hydrophilic regions may favour the adhesion of microorganisms, as reported in several food safety investigations of leafy green vegetables. Their abundance will also increase cuticular transpiration, favour foliar water uptake or decrease the shelf-life of horticultural commodities. The influence of potential factors associated with the occurrence and development of cuticular hydrophilic nano-areas in the surface of aerial organs of agro-forest species/varieties, also in response to growing conditions (e.g., environmental, plant nutrition or pest and disease control factors) or plant phenology, should be evaluated in future multidisciplinary investigations. In eco-physiological terms, the frequency of hydrophilic/hydrophobic nano-zones may significantly influence the function of plant surfaces and may be a crucial trait for adaptation to water shortage or high water pressure deficit environments.

Author Contributions

A.G.-B., G.S.-A. and V.F. conceptualised the study. A.G.-.B, G.S.-A., B.S.G.-G., T.G.-I., C.F.-R., S.M.-M., A.G.M., A.C., J.C. and V.F. carried out the investigation. A.G.-B., G.S.-A., B.S.G.-G., T.G.-I., C.F.-R., S.M.-M., A.C., A.G.M., J.C. and V.F. analysed the data. The original draft was written by A.G.-B., G.S.-A. and V.F. All the authors contributed to writing, reviewing and editing the manuscript. Funding for the development of this investigation was acquired by A.C., J.C. and V.F.

Acknowledgements

This work was supported by PID2019-104272RB-C52, PID2022-139191OB-C31 and PDC2023-145906-I00 projects, in addition to TED2021-130830B-C41, TED2021-130830B-C42 and TED2021-130830B-C43 coordinated projects which are financed by MCIN/AEI/10.13039/501100011033 and European Union NextGenerationEU/PRTR funds. G.S.-A. was supported by a María Zambrano grant (Programa de Ayudas para la Recualificación del Sistema Universitario Español) and by the 'Vicerrectoría de Investigación', Universidad Nacional, Costa Rica. Thanks to Enrique Rodríguez-Cañas (Universidad Miguel Hernández de Elche, Spain) for his support to carry out SEM analyses, and to Antonio Heredia and Eva Dominguez (Universidad de Málaga-CSIC, Spain) for helping us interpret RAMAN spectra of lettuce leaves.

Data Availability Statement

The data that support the findings of this study are available from the corresponding author upon reasonable request.

References

Almonte, L., C. Pimentel, E. Rodríguez-Cañas, J. Abad, V. Fernández, and J. Colchero. 2022. "Rose Petal Effect: A Subtle Combination of Nano-Scale Roughness and Chemical Variability." *Nano Select* 3: 977–989.

Beattie, G. A., and S. E. Lindow. 1999. "Bacterial Colonization of Leaves: A Spectrum of Strategies." *Phytopathology* 89: 353–359.

Bei, Z., X. Zhang, and X. Tian. 2023. "The Mechanism by Which Umbrella-Shaped Ratchet Trichomes on the *Elaeagnus Angustifolia* Leaf Surface Collect Water and Reflect Light." *Biology* 12, no. 7: 1024.

Bhattacharya, R., S. Saha, O. Kostina, L. Muravnik, and A. Mitra. 2020. "Replacing Critical Point Drying With a Low-Cost Chemical Drying Provides Comparable Surface Image Quality of Glandular Trichomes From Leaves of Millingtonia Hortensis L. f. in Scanning Electron Micrograph." *Applied Microscopy* 50: 15.

Blaschek, L., E. Murozuka, H. Serk, D. Ménard, and E. Pesquet. 2023. "Different Combinations of Laccase Paralogs Nonredundantly Control the Amount and Composition of Lignin in Specific Cell Types and Cell Wall Layers in Arabidopsis." *Plant Cell* 35: 889–909.

Brewer, C. A., W. K. Smith, and T. C. Vogelmann. 1991. "Functional Interaction Between Leaf Trichomes, Leaf Wettability and the Optical Properties of Water Droplets." *Plant, Cell & Environment* 14: 955–962.

Chassot, C., C. Nawrath, and J.-P. Métraux. 2007. "Cuticular Defects Lead to Full Immunity to a Major Plant Pathogen." *Plant Journal* 49: 972–980.

Chiu, Y. C., C. Shen, M. W. Farnham, and K. M. Ku. 2020. "Three-Dimensional Epicuticular Wax on Plant Surface Reduces Attachment and Survival Rate of Salmonella During Storage." *Postharvest Biology and Technology* 166: 111197.

Colchero, J., A. Storch, M. Luna, J. Gómez Herrero, and A. M. Baró. 1998. "Observation of Liquid Neck Formation With Scanning Force Microscopy Techniques." *Langmuir* 14: 2230–2234.

Dang, Q. H., and M. C. Suh. 2025. "How Plants Adapt Surface Lipids to Environmental Changes." *Nature Plants* 11: 159–160.

De Gelder, J., K. De Gussem, P. Vandenabeele, and L. Moens. 2007. "Reference Database of Raman Spectra of Biological Molecules." *Journal of Raman Specroscopy* 38: 1133–1147.

Dominguez, E., J. A. Heredia-Guerrero, and A. Heredia. 2011. "The Biophysical Design of Plant Cuticles: An Overview." *New Phytologist* 189: 938–949.

Dong, M., M. J. Holle, M. J. Miller, P. Banerjee, and H. Feng. 2024. "Fates of Attached *E. coli* o157:h7 on Intact Leaf Surfaces Revealed Leafy Green Susceptibility." *Food Microbiology* 119: 104432.

Esseili, M. A., Q. H. Wang, and L. J. Saif. 2012. "Binding of Human GII.4 Norovirus Virus-Like Particles to Carbohydrates of Romaine Lettuce Leaf Cell Wall Materials." *Applied and Environmental Microbiology* 78: 786–794.

13993054, 2025, 5, Downloaded from https://onlinelibrary.wiley.com/doi/10.1111/ppl.70580 by Victoria Fernandez - Spanish Cochrane National Provision (Ministerio de Sanidad) , Wiley Online Library on [17/10/2025]. See the Terms and Conditions (https://onlinelibrary.wiley.com/terms-and-conditions) on Wiley Online Library for rules of use; OA articles are governed by the applicable Creative Commons License

Farber, C., J. Li, E. Hager, et al. 2019. "Complementarity of Raman and Infrared Spectroscopy for Structural Characterization of Plant Epicuticular Waxes." *ACS Omega* 4: 3700–3707.

Fernández, V., L. Almonte, H. A. Bahamonde, A. Galindo-Bernabeu, G. Sáenz-Arce, and J. Colchero. 2024. "Chemical and Structural Heterogeneity of Olive Leaves and Their Trichomes." *Communications Biology* 7: 352.

Fernández, V., E. Gil-Pelegrín, and T. Eichert. 2021. "Foliar Water and Solute Absorption: An Update." *Plant Journal* 105: 870–883.

Fernández, V., P. Guzmán-Delgado, J. Graça, S. Santos, and L. Gil. 2016. "Cuticle Structure in Relation to Chemical Composition: Re-Assessing the Prevailing Model." *Frontiers in Plant Science* 7: 427.

Fernández, V., and M. Khayet. 2015. "Evaluation of the Surface Free Energy of Plant Surfaces: Toward Standardizing the Procedure." *Frontiers in Plant Science* 6: 510.

Gupta, S., C. H. Huang, G. P. Singh, B. S. Park, N.-H. Chua, and R. J. Ram. 2020. "Portable Raman Leaf-Clip Sensor for Rapid Detection of Plant Stress." *Scientific Reports* 10: 20206.

Guzmán, P., V. Fernández, J. Graça, et al. 2014. "Chemical and Structural Analysis of *Eucalyptus globulus* and *E. camaldulensis* Leaf Cuticles: A Lipidized Cell Wall Region." *Frontiers in Plant Science* 5: 481.

Hanba, Y. T., A. Moriya, and K. Kimura. 2004. "Effect of Leaf Surface Wetness and Wettability on Photosynthesis in Bean and Pea." *Plant, Cell & Environment* 27: 413–421.

Hasanuzzaman, M., K. Chakraborty, M. Zhou, and S. Shabala. 2023. "Measuring Residual Transpiration in Plants: A Comparative Analysis of Different Methods." *Functional Plant Biology* 50, no. 12: 983–992.

Hegebarth, D., C. Buschhaus, M. Wu, D. Bird, and R. Jetter. 2016. "The Composition of Surface Wax on Trichomes of *Arabidopsis thaliana* Differs From Wax on Other Epidermal Cells." *Plant Journal* 88, no. 5: 762–774.

Henningsen, J. N., M. D. Venturas, J. M. Quintero, R. R. Garrido, K. H. Mühling, and V. Fernández. 2023. "Leaf Surface Features of Maize Cultivars and Response to Foliar Phosphorus Application: Effect of Leaf Stage and Plant Phosphorus Status." *Physiologia Plantarum* 175, no. 6: e14093.

Heredia, A., J. J. Benítez, A. González Moreno, and E. Domínguez. 2024. "Revisiting Plant Cuticle Biophysics." *New Phytologist* 244: 65–73.

Heredia-Guerrero, J. A., J. J. Benítez, E. Domínguez, et al. 2014. "Infrared and Raman Spectroscopic Features of Plant Cuticles: A Review." *Frontiers in Plant Science* 5: 305.

Holloway, P. J. 1982. "Structure and Histochemistry of Plant Cuticular Membranes: An Overview." In *Plant Cuticle*, 1–32. Academic Press.

Horcas, I., R. Fernández, J. M. Gómez-Rodríguez, J. Colchero, J. Gómez-Herrero, and A. M. Baro. 2007. "WSXM: A Software for Scanning Probe Microscopy and a Tool for Nanotechnology." *Review of Scientific Instruments* 78: 13705.

Isaacson, T., D. K. Kosma, A. J. Matas, et al. 2009. "Cutin Deficiency in the Tomato Fruit Cuticle Consistently Affects Resistance to Microbial Infection and Biomechanical Properties, But Not Transpirational Water Loss." *Plant Journal* 60: 363–377.

Javelle, M., V. Vernoud, P. M. Rogowsky, and G. C. Ingram. 2011. "Epidermis: the Formation and Functions of a Fundamental Plant Tissue." *New Phytologist* 189: 17–39.

Jeffree, C. E. 2006. "The Fine Structure of the Plant Cuticle." In *Biology of the Plant Cuticle, Annual Plant Reviews*, edited by M. Riederer and C. Müller, vol. 23, 11–125. Blackwell Publishing.

Jetter, R., and M. Riederer. 2016. "Localization of the Transpiration Barrier in the Epi- and Intracuticular Waxes of Eight Plant Species: Water Transport Resistances Are Associated With Fatty Acyl Rather Than Alicyclic Components." *Plant Physiology* 170: 921–934.

Jordan, G. J., P. H. Weston, R. J. Carpenter, R. A. Dillon, and T. J. Brodribb. 2008. "The Evolutionary Relations of Sunken, Covered, and Encrypted Stomata to Dry Habitats in Proteaceae." *American Journal of Botany* 95: 521–530.

Karabourniotis, G., and G. Liakopoulos. 2006. "Phenolic Compounds in Plant Cuticles: Physiological and Ecological Aspects." *Advances in Plant Physiology* 8: 33–47.

Koch, K., B. Bhushan, and W. Barthlott. 2008. "Diversity of Structure, Morphology and Wetting of Plant Surfaces." *Soft Matter* 4: 1943–1963.

Kosma, D. K., J. A. Nemacheck, M. A. Jenks, and C. E. Williams. 2010. "Changes in Properties of Wheat Leaf Cuticle During Interactions With Hessian Fly." *Plant Journal* 63, no. 1: 31–43.

Ku, K. M., Y. C. Chiu, C. Shen, and M. Jenks. 2020. "Leaf Cuticular Waxes of Lettuce Are Associated With Reduced Attachment of the Foodborne Pathogen Salmonella spp. at Harvest and After Postharvest Storage." *LWT* 117: 108657.

Laoué, J., M. Havaux, B. Ksas, et al. 2023. "Long-Term Rain Exclusion in a Mediterranean Forest: Response of Physiological and Physico-Chemical Traits of *Quercus Pubescens* Across Seasons." *Plant Journal* 116: 1293–1308.

Lequeu, J., M.-L. Fauconnier, A. Chammaï, R. Bronner, and E. Blée. 2003. "Formation of Plant Cuticle: Evidence for the Occurrence of the Peroxygenase Pathway." *Plant Journal* 36: 155–164.

Liu, Y., A. Hanati, and H. Lan. 2023. "Characterization of Leaf Trichomes and Their Influence on Surface Wettability of *Salsola Ferganica*, an Annual Halophyte in the Desert." *Physiologia Plantarum* 175, no. 3: e13905.

Losso, A., B. Dämon, U. Hacke, and S. Mayr. 2023. "High Potential for Foliar Water Uptake in Early Stages of Leaf Development of Three Woody Angiosperms." *Physiologia Plantarum* 175, no. 4: e13961.

Lu, L., K. M. Ku, S. P. Palma-Salgado, et al. 2015. "Influence of Epicuticular Physicochemical Properties on Porcine Rotavirus Adsorption to 24 Leafy Green Vegetables and Tomatoes." *PLoS One* 10: e0132841.

Ménard, D., L. Blaschek, K. Kriechbaum, et al. 2022. "Plant Biomechanics and Resilience to Environmental Changes Are Controlled by Specific Lignin Chemistries in Each Vascular Cell Type and Morphotype." *Plant Cell* 34: 4877–4896.

Moreno, A. G., E. Domínguez, K. Mayer, et al. 2023. "3D (x-y-t) Raman Imaging of Tomato Fruit Cuticle: Microchemistry During Development." *Plant Physiology* 191: 219–232.

Natesh, H. N., L. Abbey, and S. K. Asiedu. 2017. "An Overview of Nutritional and Antinutritional Factors in Green Leafy Vegetables." *Horticulture International Journal* 1: 58–65.

Palacios-Lidón, E., B. Pérez-García, and J. Colchero. 2009. "Enhancing Dynamic Scanning Force Microscopy in Air: As Close as Possible." *Nanotechnology* 20, no. 8: 85707.

Palma-Salgado, S., K. M. Ku, M. Dong, T. H. Nguyen, J. A. Juvik, and H. Feng. 2020. "Adhesion and Removal of *E. coli* K12 as Affected by Leafy Green Produce Epicuticular Wax Composition, Surface Roughness, Produce and Bacterial Surface Hydrophobicity, and Sanitizers." *International Journal of Food Microbiology* 334: 108834.

Patwari, P., V. Salewski, K. Gutbrod, et al. 2019. "Surface Wax Esters Contribute to Drought Tolerance in Arabidopsis." *Plant Journal* 98: 727–744.

Peng, H., and I. Simko. 2023. "Extending Lettuce Shelf Life Through Integrated Technologies." *Current Opinion in Biotechnology* 81: 102951.

Pesquet, E., B. Zhang, A. Gorzsás, et al. 2013. "Non-Cell-Autonomous Postmortem Lignification of Tracheary Elements in *Zinnia elegans*." *Plant Cell* 25: 1314–1328.

13993054, 2025, 5, Downloaded from https://onlinelibrary.wiley.com/doi/10.1111/ppl.70580 by Victoria Fernandez - Spanish Cochrane National Provision (Ministerio de Sanidad) , Wiley Online Library on [17/10/2025]. See the Terms and Conditions (https://onlinelibrary.wiley.com/terms-and-conditions) on Wiley Online Library for rules of use; OA articles are governed by the applicable Creative Commons License

Philippe, G., I. Sørensen, C. Jiao, et al. 2020. "Cutin and Suberin: Assembly and Origins of Specialized Lipidic Cell Wall Scaffolds." *Current Opinion in Plant Biology* 55: 11–20.

Revilla, P., V. Fernández, L. Álvarez-Iglesias, E. T. Medina, and J. Cavero. 2016. "Leaf Physico-Chemical and Physiological Properties of Maize (*Zea mays* L.) Populations From Different Origins." *Plant Physiology and Biochemistry* 107: 319–325.

Riglet, L., S. Gatti, and E. Moyroud. 2021. "Sculpting the Surface: Structural Patterning of Plant Epidermis." *iScience* 24, no. 11: 103346.

Rosado, B. H. P., and C. D. Holder. 2013. "The Significance of Leaf Water Repellency in Ecohydrological Research: a Review." *Ecohydrology* 6: 150–161.

Roth-Nebelsick, A., V. Fernandez, J. J. Peguero-Pina, D. Sancho-Knpik, and E. Gil-Pelegrín. 2013. "Stomatal Encryption by Epicuticular Waxes as a Plastic Trait Modifying Gas Exchange in a Mediterranean Evergreen Species (*Quercus Coccifera* L.)." *Plant, Cell & Environment* 36: 579–589.

Roth-Nebelsick, A., W. Konrad, M. Ebner, T. Miranda, S. Thielen, and J. H. Nebelsick. 2022. "When Rain Collides With Plants—Patterns and Forces of Drop Impact and How Leaves Respond to Them." *Journal of Experimental Botany* 73, no. 4: 1155–1175.

Sasani, N., P. Bock, M. Felhofer, and N. Gierlinger. 2021. "Raman Imaging Reveals In-Situ Microchemistry of Cuticle and Epidermis of Spruce Needles." *Plant Methods* 17: 1–5.

Schreel, J. D., O. Leroux, W. Goossens, C. Brodersen, A. Rubinstein, and K. Steppe. 2020. "Identifying the Pathways for Foliar Water Uptake in Beech (*Fagus sylvatica* L.): A Major Role for Trichomes." *Plant Journal* 103, no. 2: 769–780.

Schulz, H., M. Baranska, and R. Baranski. 2005. "Potential of NIR-FT-Raman Spectroscopy in Natural Carotenoid Analysis." *Biopolymers* 77: 212–221.

Segado, P., E. Domínguez, and A. Heredia. 2016. "Ultrastructure of the Epidermal Cell Wall and Cuticle of Tomato Fruit (*Solanum lycopersicum* L.) During Development." *Plant Physiology* 170: 935–946.

Smith, W. K., and T. M. McClean. 1989. "Adaptive Relationship Betwenn Leaf Water Repellency, Stomatal Distribution, and Gas Exchange." *American Journal of Botany* 76: 465–469.

Suh, M. C., A. L. Samuels, R. Jetter, et al. 2005. "Cuticular Lipid Composition, Surface Structure, and Gene Expression in Arabidopsis Stem Epidermis." *Plant Physiology* 139, no. 4: 1649–1665.

Truschi, S., A. Baldi, P. Bruschi, I. Cacciari, M. Marvasi, and A. Lenzi. 2023. "Foliar Roughness and Water Content Impact on *Escherichia Coli* Attachment in Baby Leafy Greens." *Biology* 12: 102.

Veličković, D., H. Herdier, G. Philippe, D. Marion, H. Rogniaux, and B. Bakan. 2014. "Matrix-Assisted Laser Desorption/Ionization Mass Spectrometry Imaging: a Powerful Tool for Probing the Molecular Topology of Plant Cutin Polymer." *Plant Journal* 80, no. 5: 926–935.

Yadav, R. K. P., K. Karamanoli, and D. Vokou. 2005. "Bacterial Colonization of the Phyllosphere of Mediterranean Perennial Species as Influenced by Leaf Structural and Chemical Features." *Microbial Ecology* 50: 185–196.

Yeats, T. H., G. J. Buda, Z. Wang, et al. 2012. "The Fruit Cuticles of Wild Tomato Species Exhibit Architectural and Chemical Diversity, Providing a New Model for Studying the Evolution of Cuticle Function." *Plant Journal* 69: 655–666.

Yeats, T. H., and J. K. C. Rose. 2013. "The Formation and Function of Plant Cuticles." *Plant Physiology* 163: 5–20.

Zeisler-Diehl, V., Y. Müller, and L. Schreiber. 2018. "Epicuticular Wax on Leaf Cuticles Does Not Establish the Transpiration Barrier, Which Is Essentially Formed by Intracuticular Wax." *Journal of Plant Physiology* 227: 66–74.

Zivcak, M., K. Brückova, O. Sytar, M. Brestic, K. Olsovska, and S. I. Allakhverdiev. 2017. "Lettuce Flavonoids Screening and Phenotyping by Chlorophyll Fluorescence Excitation Ratio." *Planta* 245: 1215–1229.

Supporting Information

Additional supporting information can be found online in the Supporting Information section. **Figure S1:** Raman spectra of the stomatal cavity obtained (a) with 785 nm excitation (40 s. accumulation, 706 μW illumination power) and (b) with 532 nm (1 s accumulation, 110 μW power), as used for the Raman maps. The main figure in (b) shows the luminescence contribution (from 2000 to 4500 cm^{-1}) and the Raman peaks (1000–2000 cm^{-1}). The inset shows the detail of the Raman peaks' region. The raw data are depicted in red and the processed data in black (baseline subtraction for both images, 3-point polymer smooth for the processing of image [b]). The resonance enhancement obtained for the peak at 1518 cm^{-1} amounts to a factor 15. **Figure S2:** AFM images of stomata of fresh lettuce leaves. (a) 3-d image of an open stoma, and (b) 3-d image of a closed stoma. (c) AFM topography, (d) AFM wettability and (e) wettability image overlay in topography. **Figure S3:** Amplitude and phase images corresponding to the AFM topography and wettability error signal (feedback images) shown in Figure 4H.

13993054, 2025, 5, Downloaded from https://onlinelibrary.wiley.com/doi/10.1111/ppl.70580 by Victoria Fernandez - Spanish Cochrane National Provision (Ministerio de Sanidad) , Wiley Online Library on [17/10/2025]. See the Terms and Conditions (https://onlinelibrary.wiley.com/terms-and-conditions) on Wiley Online Library for rules of use; OA articles are governed by the applicable Creative Commons License